

## ARTICLE

**FeO<sub>x</sub> Coating on Pd/C Catalyst by Atomic Layer Deposition Enhances the Catalytic Activity in Dehydrogenation of Formic Acid**

Jun-jie Li, Jun-ling Lu\*

*Department of Chemical Physics, Hefei National Laboratory for Physical Sciences at the Microscale, iChEM (Collaborative Innovation Center of Chemistry for Energy Materials), CAS Key Laboratory of Materials for Energy Conversion, University of Science and Technology of China, Hefei 230026, China*

(Dated: Received on March 12, 2017; Accepted on March 27, 2017)

Hydrogen generation from formic acid (FA) has received significant attention. The challenge is to obtain a highly active catalyst under mild conditions for practical applications. Here atomic layer deposition (ALD) of FeO<sub>x</sub> was performed to deposit an ultrathin oxide coating layer to a Pd/C catalyst, therein the FeO<sub>x</sub> coverage was precisely controlled by ALD cycles. Transmission electron microscopy and powder X-ray diffraction measurements suggest that the FeO<sub>x</sub> coating layer improved the thermal stability of Pd nanoparticles (NPs). X-ray photoelectron spectroscopy measurement showed that deposition of FeO<sub>x</sub> on the Pd NPs caused a positive shift of Pd3d binding energy. In the FA dehydrogenation reaction, the ultrathin FeO<sub>x</sub> layer on the Pd/C could considerably improve the catalytic activity, and Pd/C coated with 8 cycles of FeO<sub>x</sub> showed an optimized activity with turnover frequency being about 2 times higher than the uncoated one. The improved activities were in a volcano-shape as a function of the number of FeO<sub>x</sub> ALD cycles, indicating the coverage of FeO<sub>x</sub> is critical for the optimized activity. In summary, simultaneous improvements of activity and thermal stability of Pd/C catalyst by ultra-thin FeO<sub>x</sub> overlayer suggest to be an effective way to design active catalysts for the FA dehydrogenation reaction.

**Key words:** Formic acid, Hydrogen generation, Atomic layer deposition, FeO<sub>x</sub> coating, Pd catalyst

**I. INTRODUCTION**

Hydrogen is one of the most promising energy carrier owing to its high abundance on earth and zero emission [1]. Considering the technological barriers in hydrogen storage and safety of releasing hydrogen, choosing appropriate hydrogen storage chemicals as hydrogen carriers is an attractive way for transportation [2, 3].

Among the hydrogen storage chemicals, formic acid (FA) has attracted considerable attention. FA is one of the major products formed during biomass processing [4, 5]. It is liquid at room temperature, and contains 4.4 wt% hydrogen. It is also non-toxic and can be stored safely at room temperature, which is suitable for handling and storage [4–8]. There are two possible pathways for decomposition of formic acid: the dehydrogenation pathway to form CO<sub>2</sub> and H<sub>2</sub> (HCOOH → CO<sub>2</sub> + H<sub>2</sub>), and the undesirable dehydration pathway to form H<sub>2</sub>O and CO (HCOOH → CO + H<sub>2</sub>O), in which the CO may poison the catalysts [3, 5, 9–16]. Therefore, it is highly demanded to design a catalyst with high catalytic activity and selectivity to catalyze

FA dehydrogenation to produce CO-free H<sub>2</sub> at near ambient temperature [17–24].

Among the heterogeneous catalysts used in FA dehydrogenation, Pd-based catalysts showed superior catalytic activities [19, 21, 25–29]. For instance, Zhu and co-workers synthesized the ultra-fine Pd nanoparticles (~1.4 nm) on carbon nanospheres using anhydrous methanol, and reported a turnover frequency (TOF) as high as 7256 h<sup>-1</sup> at 60 °C in the FA dehydrogenation [30]. Jiang *et al.* reported that the highly dispersed AgPd hollow spheres on the graphene (AgPd-Hs/G) showed a TOF value of 333 h<sup>-1</sup> at 25 °C, which was much higher than the Pd/G and AgPd/C catalysts. The synergistic effect between Pd and Ag and the hollow structure in which most of the atoms locate on the surface or the sub-surface of the sphere, both lead to the higher catalytic activity [31]. Xu *et al.* reported that introducing Co into AgPd bimetallic nanoparticles to form (Co<sub>6</sub>)Ag<sub>0.1</sub>Pd<sub>0.9</sub>/RGO catalyst had a significant higher TOF value of 4711 h<sup>-1</sup> at 50 °C. The promotion was attributed to the much smaller sized metal NPs by the sacrificial synthetic approach [32].

Modifying the Pd-based catalysts using metal oxide is another effective way to promote the catalytic activity in FA dehydrogenation [33–35]. Zahmakiran and co-workers reported that the presence of MnO<sub>x</sub> NPs on

\* Author to whom correspondence should be addressed. E-mail: junling@ustc.edu.cn

PdAg alloy NPs could considerably accelerate hydrogenation of FA at room temperature with a remarkable activity of  $330 \text{ mol}_{\text{H}_2} \cdot \text{mol}_{\text{catalyst}}^{-1} \cdot \text{h}^{-1}$  without any additives. The activity promotion was attributed to that  $\text{MnO}_x$  NPs provides sacrificial CO anchoring sites by forming carbonates and increasing CO poisoning tolerance, suppressing the reconstruction and leaching of Pd NPs [35]. Zhou and co-workers also found that the activities of Pd-Au/C and Pd-Ag/C catalysts could be enhanced enormously by co-deposition with  $\text{CeO}_2$ , achieving the activities as high as 1640 and  $548 \text{ mL} \cdot \text{min}^{-1} \cdot \text{g}^{-1}$  at  $91^\circ\text{C}$ , nearly 10.3 and 3.4 times higher than that of Pd-Ag/C, respectively. The activity improvement was suggested due to the formation of cationic Pd species induced by  $\text{CeO}_x$  [34].

Atomic layer deposition (ALD) is a thin film growth technique, which relies on sequential self-limiting surface reactions between gaseous precursors and a substrate. ALD can produce films in a layer-by-layer fashion at the atomic level [36, 37], thereby allowing atomic-level precise control over the coverage of oxide film on metal NPs [38–40]. Kim *et al.* reported that in the electrochemical water oxidation, the catalytic activity increased after the  $\text{TiO}_2$  ALD coating on Co/C, especially for the 60 cycle ALD( $\text{TiO}_2$ )-Co/C catalyst, which showed 2.5 times higher catalytic activity than the commercial Pt/C catalyst and was highly stable compared to Co/C [41]. In our previous work, we demonstrated that the catalytic activities of Au/ $\text{Al}_2\text{O}_3$  and Au/ $\text{SiO}_2$  in the CO oxidation increased by the ALD  $\text{TiO}_2$  coat. A volcano-like behavior of the catalytic activity as a function of the number of  $\text{TiO}_2$  ALD cycles indicated that the catalytic activities of  $\text{TiO}_2$  coated Au catalysts were highly dependent on the total length of perimeter sites [42].

Here, we precisely deposited  $\text{FeO}_x$  onto a Pd/C catalyst using ALD for different cycles to tune the coverage of  $\text{FeO}_x$ . Transmission electron microscopy (TEM) and powder X-ray diffraction (XRD) measurements showed that the ultrathin  $\text{FeO}_x$  coating layer can improve the thermal stability of Pd NPs to some extent. X-ray photoelectron spectroscopy (XPS) measurement revealed the positive shift of Pd3d binding energy owing to the strong Pd- $\text{FeO}_x$  interaction. In FA dehydrogenation, we found the ultrathin  $\text{FeO}_x$  layer on the Pd/C catalyst could considerably improve the catalytic activity, and the coverage of  $\text{FeO}_x$  over layer on Pd NPs is very critical for the optimized activity.

## II. EXPERIMENTS

### A. Pd/C catalyst synthesis

The Pd/C catalyst was prepared using sodium borohydride ( $\text{NaBH}_4$ , 96%, Sinopharm Chemical Reagent Co. Ltd.) as a reducing agent, and sodium citrate (Sinopharm Chemical Reagent Co. Ltd.) as a sta-

bilizing agent according to a procedure reported previously [43]. Carbon black (Vulcan XC72R, Carbot Corp.) was used as the catalyst support as received. Typically, the Pd/C catalyst was synthesized as follows: 0.1 mmol  $\text{PdCl}_2$  (dissolved in 0.1 mol/L HCl solution) and 0.8 mmol sodium citrate was dissolved into 150 mL water. 400 mg carbon black was then added. After stirring the mixture for 20 min, followed by 30 min sonication, 15 mL of 0.1 mol/L  $\text{NaBH}_4$  solution was added drop wise into the suspension under vigorous stirring; and the solution was further stirred at  $25^\circ\text{C}$  for another 8 h. Next, the precipitate was filtered, and washed with deionized water for several times to remove the weakly bonded sodium citrate agent. The obtained materials were then dried overnight in a vacuum oven at  $40^\circ\text{C}$  to obtain the Pd/C catalyst.

### B. $\text{FeO}_x$ ALD coating

$\text{FeO}_x$  ALD was carried out on a viscous flow reactor (GEMSTAR-6<sup>TM</sup> Benchtop ALD, Arradance) at  $150^\circ\text{C}$  by alternatively exposing ferrocene (99.7%, Sigma-Aldrich) and ultrahigh purity oxygen (99.999%) for different ALD cycles [44]. The ferrocene precursor contained in a stainless steel reservoir was heated up to  $90^\circ\text{C}$  to get a reasonable vapor pressure and the inlet lines were heated to  $120^\circ\text{C}$  to avoid any condensation. Ultrahigh purity  $\text{N}_2$  (99.999%) was used as carrier gas at a flow rate of 200 mL/min.  $\text{FeO}_x$  ALD was executed on the Pd/C catalyst using the timing sequence of 90, 200, 120, and 200 s for ferrocene exposure,  $\text{N}_2$  purge,  $\text{O}_2$  exposure and  $\text{N}_2$  purge, respectively. The Pd/C sample with different ALD cycles of  $\text{FeO}_x$  was expressed as  $x\text{FePd/C}$ , where  $x$  is denoted as the number of  $\text{FeO}_x$  ALD cycles.

### C. Characterization

The loadings of Pd and Fe were determined by an inductively coupled plasma atomic emission spectrometer (ICP-AES). The morphologies of the Pd/C catalysts were characterized by TEM (JEOL-2010) at 200 kV. Powder XRD measurements were carried out on a Philips X'Pert Pro Super diffractometer at the Structure Research Center at University of Science and Technology of China, with a  $\text{Cu K}\alpha$  radiation ( $\lambda=1.5418 \text{ \AA}$ ), operated at 40 kV and 50 mA. XPS measurements were taken on a Thermo-VG Scientific Escalab 250 spectrometer, equipped with an aluminum anode (Al  $\text{K}\alpha=1486.6 \text{ eV}$ , Hefei University of Technology).

### D. Catalytic activity

All the catalysts were pretreated at  $250^\circ\text{C}$  in 10%  $\text{O}_2$  in Ar for 1 h and  $300^\circ\text{C}$  in 10%  $\text{H}_2$  in Ar for 1 h be-

fore catalytic performance test. The catalytic activities of the Pd/C catalysts in FA decomposition were evaluated in a gas generation setup, which can be found elsewhere [45, 46]. In brief, the catalyst and the FA (98%, Sinopharm Chemical Reagent Co. Ltd.)/sodium formate (SF, 99.5%, Sinopharm Chemical Reagent Co. Ltd) aqueous solution were loaded into a two-necked round-bottomed flask (50 mL), which was placed in a water bath at 25 °C under an ambient atmosphere. A gas burette filled with water was connected with the reaction flask to measure the volume of released gas. Typically, 55 mg catalyst was first loaded into the reaction flask, and 5 mL FA substrate solution containing FA (0.6 mol/L) and SF (0.6 mol/L) was then added under vigorously stirring. The volume of the generated gas was immediately monitored by recording the displacement of water in the gas burette against reaction time. Here general TOF values were calculated as the following equation [17, 30, 32]:

$$\text{TOF} = \frac{n_{\text{gas}}}{2n_{\text{Pd}}} \cdot \frac{1}{t} \quad (1)$$

Here  $n_{\text{gas}}$  is the mole number of generated gas at a conversion below 20%,  $n_{\text{Pd}}$  is the mole number of Pd atoms,  $t$  is the reaction time.

### E. On-line gas chromatography measurements

The gas burette was disconnected from the reaction flask and replaced by an argon (Ar) gas line. Meanwhile, a gas outlet from the flask was connected to an online gas chromatography instrument (GC, Shimadzu GC-2014) equipped with a flame ionization detector (FID) along with a methanator as well as a thermal conductivity detector (TCD). After the reaction started, Ar was bubbled into the reaction solution at a flow rate of 15 mL/min, and the generated gas was carried to the GC for analysis. A reference mixture gas containing 1% CO and 1% CO<sub>2</sub> in Ar was also recorded for comparison.

## III. RESULTS AND DISCUSSION

### A. Morphology of catalysts

The loading of Pd and Fe in the catalysts are shown in Table I. TEM measurement was employed to characterize the morphologies of these catalysts as shown in FIG. 1. Besides the dominant Pd NPs with a size of ~3.1 nm, a considerable number of Pd NPs with a larger size of ~6.3 nm were also frequently observed in the uncoated Pd/C catalyst (FIG. 1(a)). These larger Pd NPs were likely formed through aggregation during the high temperature pretreatment. In contrast, the Pd particle size was rather similar, about 3.6 nm, highly dispersed in the 5cFePd/C, 8cFePd/C and 12cFePd/C

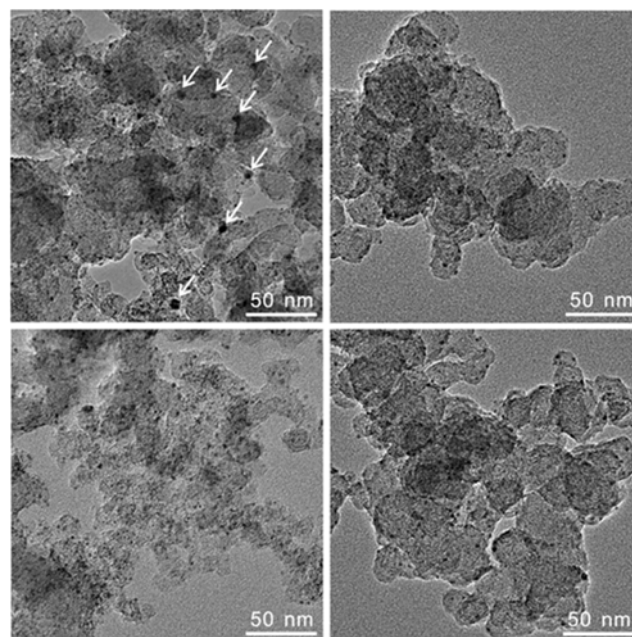


FIG. 1 TEM images of (a) Pd/C, (b) 5cFePd/C, (c) 8cFePd/C, and (d) 12cFePd/C catalysts after calcination at 250 °C for 1 h and then reduction at 300 °C for another 1 h. White arrows highlight the Pd NPs with significant large sizes.

TABLE I The Pd and Fe loadings in these catalysts determined by ICP-AES.

Samples	Pd loading/wt%	Fe loading/wt%
8cFe/C	—	0.98
Pd/C	2.3	—
2cFePd/C	2.3	0.48
5cFePd/C	2.3	0.94
8cFePd/C	2.3	1.13
12cFePd/C	2.3	1.31

samples (FIG. 1 (b)–(d)). Obviously, the FeO<sub>x</sub> coating layer on the Pd NPs improved the thermal stability of Pd NPs against sintering, although the FeO<sub>x</sub> was extremely thin and could not be observed by TEM under current resolution [44].

XRD measurements were further performed on these samples. As shown in FIG. 2, a broad diffraction peak at ~26° can be observed on all the samples, which can be attributed to the C(002) diffraction peak from the carbon black support [47]. Sharp diffraction peaks at 40.1° and 46.8°, which can be assigned to the (111) and (200) of Pd, indicating the presence of large size of Pd NPs on the uncoated Pd/C sample [43]. However, no visible diffraction peaks of Pd can be found on the 2cFePd/C, 5cFePd/C, 8cFePd/C, and 12cFePd/C samples, indicating ultrafine Pd NPs were highly dispersed on the C support [48]. These results were consistent well with the TEM images.

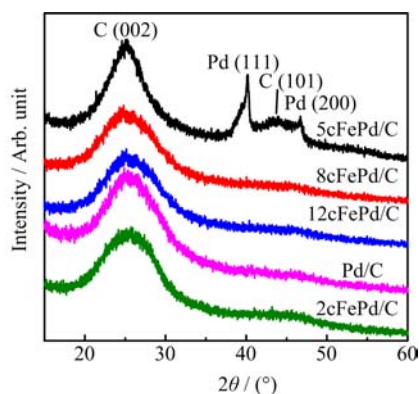


FIG. 2 XRD patterns of Pd/C and  $x$ cFePd/C catalysts.

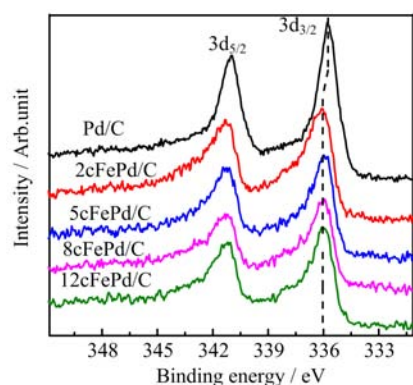


FIG. 3 XPS spectra of the Pd/C, 2cFePd/C, 5cFePd/C, 8cFePd/C, and 12cFePd/C catalysts in the Pd3d region.

## B. XPS studies

XPS was carried out to study the electronic properties of the Pd NPs in these samples in the Pd3d region as shown in FIG. 3. The binding energy of Pd3d<sub>5/2</sub> on the uncoated Pd/C sample was 335.8 eV, which is assigned to the zero-valence Pd [49, 50]. After depositing FeO<sub>x</sub> on Pd/C by ALD, the Pd3d binding energy shifted to a higher value of ~336.1 eV owing to the strong Pd-FeO<sub>x</sub> interaction, confirming the successful deposition of FeO<sub>x</sub> on Pd NPs. The positive shift of Pd3d binding energy by the FeO<sub>x</sub> coating layer implies that the Pd was electron deficient on the  $x$ cFePd/C samples [51–54].

## C. Catalytic activity

The activities of Pd/C and  $x$ cFePd/C catalysts were evaluated in FA dehydrogenation in a FA/SF aqueous solution at 25 °C under ambient atmosphere. As shown in FIG. 4(a), the 8cFe/C sample without presence of Pd did not show any catalytic activity, indicating the FeO<sub>x</sub> itself had no contribution to the FA dehydrogenation reaction. On the other hand, the uncoated Pd/C generated about 70 mL gas (CO<sub>2</sub>+H<sub>2</sub>) in 80 min. The

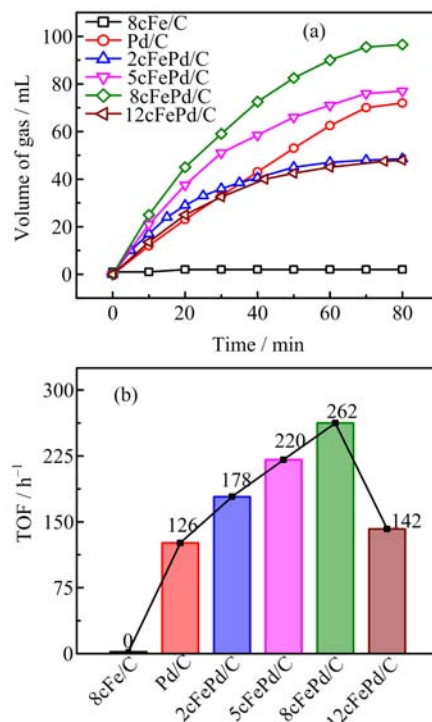


FIG. 4 (a) Plots of the volume of the generated gases (CO<sub>2</sub>+H<sub>2</sub>) versus time over the Pd/C catalysts with and without the FeO<sub>x</sub> coating. (b) Calculated TOFs of catalysts based on the amount of Pd. Reaction conditions: 5 mL aqueous solution of 0.6 mol/L FA+0.6 mol/L SF, 55 mg catalyst, reaction temperature: 25 °C. The solid line in (b) is used to guide eyes.

initial activity of 2cFePd/C was higher than the uncoated Pd/C sample, but it quickly slowed down and generated 50 mL gas in 80 min. The activity was further improved as increasing the coverage of FeO<sub>x</sub>, and the maximum activity was achieved on 8cFePd/C by generating 100 mL gas. Further increasing the number of FeO<sub>x</sub> ALD cycles to 12 (12cFePd/C) resulted a significant activity drop.

We further calculated the initial TOFs based on the moles of Pd. The uncoated Pd/C showed an initial TOF of 126 h<sup>-1</sup>, which was in agreement with the previous work [55]. After depositing different cycles of FeO<sub>x</sub> on Pd/C by ALD, considerable improvement of catalytic activity was observed, and the TOF values were 178, 220, 262, and 142 h<sup>-1</sup> for the 2cFePd/C, 5cFePd/C, 8cFePd/C, and 12cFePd/C, respectively. A clear volcano-shape of the catalytic activity as a function of the number of FeO<sub>x</sub> ALD cycles was observed. The activity promotion by FeO<sub>x</sub> might be related with the electronic modulation of Pd as observed by XPS shown in FIG. 3, in line with the previous observation on CeO<sub>x</sub> promoted Pd-Au/C and Pd-Ag/C catalysts, where the formation of cationic Pd species was suggested to be responsible for the activity promotion [34]. On the other hand, the formed Pd-FeO<sub>x</sub> interface might

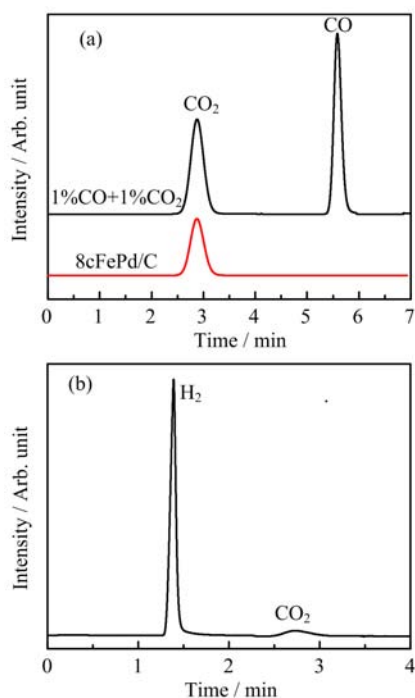


FIG. 5 Online GC spectra of the generated gas from the FA/SF solution over the 8cFePd/C catalyst at 25 °C using either (a) FID-methanator or (b) TCD. The reference mixture gas of 1%CO and 1%CO<sub>2</sub> balanced in Ar was also shown in (a) for comparison.

also play a certain role in the activity enhancement. The sharp catalytic activity decrease in the 12cFePd/C sample may be caused by the excessive FeO<sub>x</sub> coating which blocks significantly Pd surface active sites and leads to the decrease of catalytic activity in FA dehydrogenation, indicating an appropriate FeO<sub>x</sub> coverage is very critical for the activity promotion.

#### D. Composition of generated gas

In FA dehydrogenation, a low level of CO may be formed via the dehydration path way (HCOOH → CO + H<sub>2</sub>O). The undesired CO can severely poison the Pd catalysts and lead to catalyst deactivation [3, 5, 9–16]. To determine whether the CO product was released in the gaseous products during the reaction, *in situ* monitoring of the composition of the released gas by an online GC was carried out on the 8cFePd/C catalyst. As shown in FIG. 5(a), only the CO<sub>2</sub> peak can be observed by a FID-methanator detector, compared to the reference mixture gas (1%CO and 1%CO<sub>2</sub>). Clearly the formation of CO in FA dehydrogenation was negligible, below the detection level even with a FID-methanator detector. On the other hand, using a TCD detector, we clearly observed H<sub>2</sub> and CO<sub>2</sub> in the released gas as shown in FIG. 5(b). Therefore, the FA dehydrogenation path to CO<sub>2</sub> and H<sub>2</sub> formation was dominant on

8cFePd/C during the reaction.

#### IV. CONCLUSION

In this work, FeO<sub>x</sub> ALD was performed on a Pd/C catalyst to precisely deposit an oxide coating layer to the Pd NPs. According to the TEM and XRD results, we found that the FeO<sub>x</sub> coating layer can improve the thermal stability of Pd NPs to some extent. The XPS measurement confirmed the successful deposition of FeO<sub>x</sub> on the Pd NPs, as the binding energy shifted to a higher value at 336.1 eV in the Pd 3d<sub>5/2</sub> via the strong interaction between the FeO<sub>x</sub> layer and Pd NPs. In the FA dehydrogenation reaction, the improvement of catalytic activity in a volcano-shape as a function of the number of FeO<sub>x</sub> ALD cycles was observed, and the 8cFePd/C sample showed a highest activity of 262 h<sup>-1</sup> at room temperature, which was about 2 times higher than the uncoated Pd/C. The activity promotion by FeO<sub>x</sub> is likely correlated with the electronic modulation of Pd and the formed Pd-FeO<sub>x</sub> interfaces. Taken together, we achieved considerable improvement of thermal stability and activity of Pd catalyst simultaneously by carefully controlling the coverage of FeO<sub>x</sub> coating layer.

#### V. ACKNOWLEDGMENTS

This work was supported by the National Natural Science Foundation of China (No.51402283 and No.21473169), One Thousand Young Talents Program under the Recruitment Program of Global Experts, the Fundamental Research Funds for the Central Universities (No.WK2060030017), and the Startup Funds from University of Science and Technology of China.

- [1] S. Young, *Nature* **414**, 487 (2001).
- [2] A. Boddien, B. Loges, F. Gärtner, C. Torborg, K. Fumino, H. Junge, R. Ludwig, and M. Beller, *J. Am. Chem. Soc.* **132**, 8924 (2010).
- [3] M. Yadav and Q. Xu, *Energ Environ. Sci.* **5**, 9698 (2012).
- [4] D. T. Whipple and P. J. A. Kenis, *J. Phys. Chem. Lett.* **1**, 3451 (2010).
- [5] M. Grasemann and G. Laurenczy, *Energ Environ. Sci.* **5**, 8171 (2012).
- [6] W. H. Wang, M. G. Niu, Y. C. Hou, W. Z. Wu, Z. Y. Liu, Q. Y. Liu, S. H. Ren, and K. N. Marsh, *Green Chem.* **16**, 2614 (2014).
- [7] A. Boddien, F. Gärtner, C. Federsel, P. Sponholz, D. Mellmann, R. Jackstell, H. Junge, and M. Beller, *Angew. Chem. Int. Ed.* **50**, 6411 (2011).
- [8] K. Tedsree, T. Li, S. Jones, C. W. A. Chan, K. M. K. Yu, P. A. J. Bagot, E. A. Marquis, G. D. W. Smith, and S. C. E. Tsang, *Nat. Nanotechnol.* **6**, 302 (2011).

- [9] F. Joo, *ChemSusChem* **1**, 805 (2008).
- [10] B. Loges, A. Boddien, H. Junge, and M. Beller, *Angew. Chem. Int. Ed.* **47**, 3962 (2008).
- [11] Z. L. Liu, L. Hong, M. P. Tham, T. H. Lim, and H. X. Jiang, *J. Power Sources* **161**, 831 (2006).
- [12] P. Gruene, A. Fielicke, G. Meijer, and D. M. Rayner, *Phys. Chem. Chem. Phys.* **10**, 6144 (2008).
- [13] C. Lamy, A. Lima, V. LeRhun, F. Delime, C. Coutanceau, and J. M. Leger, *J. Power Sources* **105**, 283 (2002).
- [14] V. Bambagioni, C. Bianchini, A. Marchionni, J. Filippi, F. Vizza, J. Teddy, P. Serp, and M. Zhiani, *J. Power Sources* **190**, 241 (2009).
- [15] Y. Xu, A. V. Ruban, and M. Mavrikakis, *J. Am. Chem. Soc.* **126**, 4717 (2004).
- [16] A. Boddien, B. Loges, H. Junge, and M. Beller, *ChemSusChem* **1**, 751 (2008).
- [17] K. Jiang, K. Xu, S. Zou, and W. B. Cai, *J. Am. Chem. Soc.* **136**, 4861 (2014).
- [18] F. Z. Song, Q. L. Zhu, N. Tsumori, and Q. Xu, *ACS Catal.* **5**, 5141 (2015).
- [19] C. Hu, X. Mu, J. Fan, H. Ma, X. Zhao, G. Chen, Z. Zhou, and N. Zheng, *ChemNanoMat* **2**, 28 (2016).
- [20] S. J. Li, Y. Ping, J. M. Yan, H. L. Wang, M. Wu, and Q. Jiang, *J. Mater. Chem. A* **3**, 14535 (2015).
- [21] N. Cao, S. Tan, W. Luo, K. Hu, and G. Cheng, *Catal. Lett.* **146**, 518 (2015).
- [22] D. W. Lee, M. H. Jin, Y. J. Lee, J. H. Park, C. B. Lee, and J. S. Park, *Sci. Rep.* **6**, 26474 (2016).
- [23] A. Boddien, D. Mellmann, F. Gartner, R. Jackstell, H. Junge, P. J. Dyson, G. Laurenczy, R. Ludwig, and M. Beller, *Science* **333**, 1733 (2011).
- [24] Q. Y. Bi, X. L. Du, Y. M. Liu, Y. Cao, H. Y. He, and K. N. Fan, *J. Am. Chem. Soc.* **134**, 8926 (2012).
- [25] K. Mori, M. Dojo, and H. Yamashita, *ACS Catal.* **3**, 1114 (2013).
- [26] J. S. Yoo, Z. J. Zhao, J. K. Nørskov, and F. Studt, *ACS Catal.* **5**, 6579 (2015).
- [27] Z. L. Wang, J. M. Yan, Y. Ping, H. L. Wang, W. T. Zheng, and Q. Jiang, *Angew. Chem. Int. Ed.* **52**, 4406 (2013).
- [28] Y. J. Huang, X. C. Zhou, M. Yin, C. P. Liu, and W. Xing, *Chem. Mater.* **22**, 5122 (2010).
- [29] J. Cheng, X. J. Gu, X. L. Sheng, P. L. Liu, and H. Q. Su, *J. Mater. Chem. A* **4**, 1887 (2016).
- [30] Q. L. Zhu, N. Tsumori, and Q. Xu, *J. Am. Chem. Soc.* **137**, 11743 (2015).
- [31] Y. Jiang, X. Fan, X. Xiao, T. Qin, L. Zhang, F. Jiang, M. Li, S. Li, H. Ge, and L. Chen, *J. Mater. Chem. A* **4**, 657 (2016).
- [32] Y. Chen, Q. L. Zhu, N. Tsumori, and Q. Xu, *J. Am. Chem. Soc.* **137**, 106 (2015).
- [33] Y. Karatas, A. Bulut, M. Yurderi, I. E. Ertas, O. Alal, M. Gulcan, M. Celebi, H. Kivrak, M. Kaya, and M. Zahmakiran, *Appl. Catal. B* **180**, 586 (2016).
- [34] X. Zhou, Y. Huang, W. Xing, C. Liu, J. Liao, and T. Lu, *Chem. Commun.* **30**, 3540 (2008).
- [35] A. Bulut, M. Yurderi, Y. Karatas, Z. Say, H. Kivrak, M. Kaya, M. Gulcan, E. Ozensoy, and M. Zahmakiran, *ACS Catal.* **5**, 6099 (2015).
- [36] J. L. Lu, J. W. Elam, and P. C. Stair, *Acc. Chem. Res.* **46**, 1806 (2013).
- [37] C. L. Wang and J. L. Lu, *Chin. J. Chem. Phys.* **29**, 571 (2016).
- [38] J. L. Lu, B. S. Fu, M. C. Kung, G. M. Xiao, J. W. Elam, H. H. Kung, and P. C. Stair, *Science* **335**, 1205 (2012).
- [39] X. H. Liang, J. H. Li, M. Yu, C. N. McMurray, J. L. Falconer, and A. W. Weimer, *ACS Catal.* **1**, 1162 (2011).
- [40] H. Feng, J. L. Lu, P. C. Stair, and J. W. Elam, *Catal. Lett.* **141**, 512 (2011).
- [41] H. J. Kim, D. H. K. Jackson, J. Lee, Y. X. Guan, T. F. Kuech, and G. W. Huber, *ACS Catal.* **5**, 3463 (2015).
- [42] C. L. Wang, H. W. Wang, Q. Yao, H. Yan, J. J. Li, and J. L. Lu, *J. Phys. Chem. C* **120**, 478 (2016).
- [43] D. F. Gao, H. Zhou, J. Wang, S. Miao, F. Yang, G. X. Wang, J. G. Wang, and X. H. Bao, *J. Am. Chem. Soc.* **137**, 4288 (2015).
- [44] H. Yi, H. Y. Du, Y. L. Hu, H. Yan, H. L. Jiang, and J. L. Lu, *ACS Catal.* **5**, 2735 (2015).
- [45] Y. Yamada, K. Yano, and S. Fukuzumi, *Energy Environ. Sci.* **5**, 5356 (2012).
- [46] H. L. Jiang and Q. Xu, *Catal. Today* **170**, 56 (2011).
- [47] T. Xu, H. M. Zhang, H. X. Zhong, Y. W. Ma, H. Jin, and Y. N. Zhang, *J. Power Sources* **195**, 8075 (2010).
- [48] W. J. Shen and Y. Matsumura, *J. Mol. Catal. A* **153**, 165 (2000).
- [49] H. W. Wang, C. L. Wang, H. Yan, H. Yi, and J. L. Lu, *J. Catal.* **324**, 59 (2015).
- [50] W. P. Zhou, A. Lewera, R. Larsen, R. I. Masel, P. S. Bagus, and A. Wieckowski, *J. Phys. Chem. B* **110**, 13393 (2006).
- [51] Y. S. Bi, L. Chen, and G. X. Lu, *J. Mol. Catal. A* **266**, 173 (2007).
- [52] N. S. Babu, N. Lingaiah, J. V. Kumar, and P. S. S. Prasad, *Appl. Catal. A* **367**, 70 (2009).
- [53] M. P. Felicissimo, O. N. Martyanov, T. Risse, and H. J. Freund, *Surf. Sci.* **601**, 2105 (2007).
- [54] R. Muftikian, K. Nebesny, Q. Fernando, and N. Korte, *Environ. Sci. Technol.* **30**, 3593 (1996).
- [55] Z. L. Wang, J. M. Yan, H. L. Wang, Y. Ping, and Q. Jiang, *Sci. Rep.* **2**, 598 (2012).